Gas Separation by High-Flux, Asymmetric Hollow-Fiber Membrane

A mathematical model of multicomponent permeation systems with high-flux, asymmetric hollow-fiber membranes is presented. The model takes into account the permeate pressure variation inside the fiber. In the special case of negligible permeate pressure drop, the model yields a simple analytical solution for membrane area calculation that eliminates the numerical integration step required in existing methods. Laboratory multicomponent permeation experiments have verified the mathematical model and have demonstrated the technical feasibility of using the high-flux asymmetric cellulose acetate hollow fiber for H_2, CO_2, and H_2S separation. It is shown that the selectivity of the cellulose acetate membrane is ideally suited to the recovery of hydrogen from the purge gas of reactor recycle loops. For the separation of high-concentration CO_2 or H_2S, the test data show that the permeabilities of the individual components in mixed gas permeation are significantly different from those of pure gases.

C. Y. Pan
Alberta Research Council
Edmonton, Alberta, Canada

Introduction

Selective permeation through a membrane is an increasingly important technique for gas separation. The recent development of asymmetric hollow-fiber and composite membranes, in which separation takes place in an ultrathin skin of selective polymers over a porous supporting layer, makes it possible to have both high permeability and high selectivity for efficient gas separation. The process is technically simple and the equipment is compact and modular. In the case of hollow-fiber membranes, the permeator module is constructed similar to the shell-and-tube type heat exchanger, and thousands of square feet of membrane area can be packed into one cubic foot (0.03 m^3) of pressure vessel volume. The high-pressure feed gas is usually directed through the shell side of the permeator, and permeate that is enriched with the more permeable components is withdrawn from the inside of the fibers through the openings on the fiber tube sheet.

The performance of the permeator for gas separation depends not only on membrane permeability and selectivity, but also on membrane structure. For the conventional symmetric membrane, which has a homogeneous structure with uniform permeation properties across its entire thickness, gas separation performance is strongly dependent on the feed and permeate flow pattern (cross-flow, countercurrent, or cocurrent). For the asymmetric membrane, however, gas separation performance is virtually independent of the flow pattern. This is because the porous supporting layer prevents the mixing of local permeate fluxes, giving rise to a cross-flow pattern with respect to the membrane skin, irrespective of the flow direction of the bulk permeate stream outside the porous layer (Pan, 1983). In this paper a mathematical model and experimental results of multicomponent permeation systems with high-flux, asymmetric hollow-fiber membranes are presented.

Mathematical Model of Multicomponent Permeation

Various mathematical models and calculation methods for the conventional symmetric membrane have been reported in the literature (Blaisdell and Kammermeyer, 1972, 1973; Boucif et al., 1983; Chern et al., 1983a; Haraya et al., 1985; Hwang and Kammermeyer, 1975; Oishi et al., 1961; Pan and Habgood, 1974, 1978a,b; Perrin and Stern, 1985; Saltonstall et al., 1983; Shindo et al., 1985; Stern, 1972; Stern and Wang, 1978; Thorman et al., 1975; Walawender and Stern, 1972; Weller and Steiner, 1950a,b). For the high-flux, asymmetric membrane, Pan (1983) reported a model of the binary permeation system and analyzed the effect of permeate pressure buildup inside the fiber bore on gas separation performance. In the following, a

mathematical model of the multicomponent permeation system with asymmetric hollow-fiber membranes is presented.

Figure 1 illustrates the permeation of a gas mixture through an asymmetric hollow-fiber membrane. The concentration of the local permeate stream leaving the membrane skin, y_i, is generally different from that of the bulk permeate stream, $\bar{y}_i$. For membranes with an ultrathin skin and a highly porous supporting layer, the effect of back-diffusion from $\bar{y}_i$ to y_i is negligible. This is the key assumption of the mathematical model presented here. Other relevant assumptions are as follows:

1. The deformation of the hollow fiber under pressure is negligible.
2. Membrane permeabilities are independent of pressure and concentration.
3. The high-pressure feed gas is on the skin side of the membrane and has negligible pressure drop.
4. The permeate pressure drop can be calculated by the Hagen-Poiseuille equation (Berman, 1953).

Subject to the above assumptions, the permeation of a multicomponent gas mixture through the asymmetric hollow fiber may be described by the following set of equations.

$$\frac{d(ux_i)}{dz} = -\pi D_o N(Q_i/d)(Px_i - py_i) \quad i = 1, n \tag{1}$$

$$\frac{d(ux_i)}{du} = y_i \quad i = 1, n \tag{2}$$

$$\frac{dp^2}{dz} = \frac{-256RT\mu v}{\pi D_i^4 N} \tag{3}$$

Equations 1–3 are applicable to both cocurrent and countercurrent flow patterns. In either case, the feed flow is considered to be in the direction of positive values of z. Thus, for the countercurrent mode it is necessary to assign negative values to the permeate flow, v, in Eq. 3. To facilitate the solution of these equations, we seek to separate the concentration variables from the flow rate and membrane area, and to reduce the number of differential equations to be integrated simultaneously. Dividing Eq. 1 by (Q_i/d), and then taking the sum of the resulting equations for each component yields

$$\sum_1^n \frac{d(Ux_i)}{\alpha_i dS} = -(1 - \gamma) \tag{4}$$

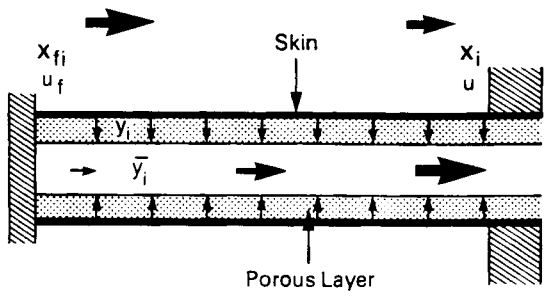

Figure 1. Gas permeation through asymmetric hollow-fiber membrane.

where

$$U = u/u_f$$

$$S = \pi D_o z N P(Q_1/d)/u_f$$

$$\gamma = p/P$$

Equation 2 may be written as

$$d(\ln U) = \frac{dx_i}{y_i - x_i} \tag{5}$$

Substituting the relation for $d(ux_i)$ given by Eq. 2 into Eqs. 1 and 4 yields

$$\frac{dU}{dS} = \frac{-\alpha_i(x_i - \gamma y_i)}{y_i} = \frac{-(1 - \gamma)}{y_o} \tag{6}$$

where

$$y_o = \sum_1^n y_i/\alpha_i$$

From the second equality of Eq. 6, we obtain the following equations relating the local permeate concentrations to the feed-side concentrations.

$$x_i = \gamma y_i + \frac{(1 - \gamma)y_i}{\alpha_i y_o} \tag{7}$$

$$y_i = \frac{\alpha_i x_i y_o}{1 - \gamma + \gamma\alpha_i y_o} \tag{8}$$

$$\sum_1^n \frac{\alpha_i x_i y_o}{1 - \gamma + \gamma\alpha_i y_o} = 1 \tag{9}$$

Substituting Eq. 7 into Eq. 5 yields

$$d(\ln U) = \frac{1 + \gamma(\alpha_i y_o - 1)}{(1 - \gamma)(\alpha_i y_o - 1)} \frac{dy_i}{y_i} - \frac{dy_o}{y_o(\alpha_i y_o - 1)} + \frac{d\gamma}{1 - \gamma} \tag{10}$$

Combining the two member equations of Eq. 10 for components i and n, we obtain an expression for dy_i in terms of dy_o and dy_n. Taking the sum of this expression for $i = 1$ to n, we obtain another expression for dy_o in terms of dy_n. Eliminating dy_o from these two expressions yields

$$\frac{dy_i}{dy_n} = \frac{y_i}{y_n}\left(A_i - \frac{B_i \sum_1^n A_j y_j}{\sum_1^n B_j y_j}\right) \quad i = 2, n - 1 \tag{11}$$

where

$$A_i = (\alpha_i y_o - 1)(1 - \gamma + \gamma\alpha_n y_o)/[(\alpha_n y_o - 1)(1 - \gamma + \gamma\alpha_i y_o)]$$

$$B_i = (1 - \gamma)(\alpha_n - \alpha_i)/[(\alpha_n y_o - 1)(1 - \gamma + \gamma\alpha_i y_o)]$$

Integrating Eq. 6 from the feed inlet end yields

$$S = -\int_1^U \frac{y_o}{1 - \gamma} dU \tag{12}$$

It can be shown by material balance that the permeate flow variable v in Eq. 3 is equal to $u_c - u$, where the subscript c refers to the closed end of the hollow fiber. Thus, Eq. 3 may be written as

$$\frac{d\gamma^2}{dS} = -C(\mu/\mu_1)/(U_c - U) \tag{13}$$

where

$$C = \frac{256RT\mu_1 u_f^2}{\pi^2 N^2 D_o D_i^4 P^3 (Q_1/d)}$$

Equations 7–13 are now the governing equations for the multicomponent permeation system. Equations 7–9 relate the variables y_i to x_i and vice versa. Given the local permeate composition y_i's at any point on the membrane, the corresponding feed-side composition can be calculated by Eq. 7. Conversely, if x_i's are known, y_i's can be calculated by Eq. 8 using the value of y_o obtained by solving Eq. 9.

The integration of Eqs. 10–13 is always of the boundary value problem due to the unknown permeate pressure profile inside the fiber. A trial-and-error shooting method is generally required to obtain the solution. However, for the practical problem of calculating the performance of a given membrane module with specified feed pressure and composition, concentration of one component in the residue, and permeate pressure at the fiber opening, a straightforward iteration method may be used to obtain the solution. Based on an arbitrarily assumed permeate pressure profile (e.g., uniform permeate pressure), the composition and flow profiles (i.e., the relationship between composition, flow, and dimensionless membrane area) can be calculated by integrating Eqs. 11, 10, and 12, respectively and sequentially. These profiles are in turn used to generate a new permeate pressure profile by Eq. 13. (The feed flow u_f in the constant, C, of Eq. 13 can be calculated from the dimensionless membrane area, S, obtained from Eq. 12.) Improved composition and flow profiles are then calculated based on the corrected permeate pressure profile and vice versa, until all profiles converge to their respective limits. The bulk permeate composition $\bar{y}_i$'s at the fiber outlet can be calculated by material balances from the compositions and flows of the feed and residue streams. The above method of solution is applicable to both countercurrent and cocurrent flow patterns. In either case, the integration of Eqs. 10–12 is started at the feed inlet end with the initial values of y_i's calculated from the given feed composition using Eq. 8 with the aid of y_o determined by Eq. 9. The integration of Eq. 13, however, is always started at the fiber opening end where the permeate outlet pressure is given. Finally, it is important to note that the component n should be the most or the least permeable component, to ensure that the differential dy_n in the denominator of Eq. 11 will not vanish.

Permeation systems with constant permeate pressure

For the special case of negligible permeate pressure drop inside the fiber, Eq. 13 is not needed and Eqs. 7–12 are applicable not only to the asymmetric membrane in any flow pattern, but also to the symmetric membrane in the cross-flow mode. In this case, the above iteration procedure is not required, and the compositions and flows can be calculated by straightforward integration of Eqs. 11 and 10, respectively, from the feed inlet end. A simple solution for the membrane area can readily be obtained from Eq. 4. With γ = constant, Eq. 4 can be integrated from the feed inlet to any point on the membrane surface to give

$$S = \frac{1}{1 - \gamma} \sum_1^n \frac{x_{fi} - Ux_i}{\alpha_i} \tag{14}$$

This equation may be written in terms of the bulk permeate concentration $\bar{y}_i$ and stage cut θ as follows:

$$S = \frac{\theta}{1 - \gamma} \sum_1^n \frac{\bar{y}_i}{\alpha_i} \tag{15}$$

where

$$\bar{y}_i = (x_{fi} - Ux_i)/(1 - U)$$

$$\theta = 1 - U$$

Using the values of the stage cut and bulk permeate composition obtained by solving Eqs. 10 and 11, the membrane area can easily be calculated by Eq. 15. For the binary system, Eq. 15 may be used in conjunction with the composition and stage cut calculated by the Weller and Steiner (1950a) solution, or the following equations (Pan and Habgood, 1978a):

$$U = \left(\frac{y_2}{y_{f2}}\right)^a \left(\frac{1 - y_2}{1 - y_{f2}}\right)^b \left[\frac{\alpha_2 - (\alpha_2 - 1)y_2}{\alpha_2 - (\alpha_2 - 1)y_{f2}}\right] \tag{16}$$

where

$$y_2 = \frac{1 + (\alpha_2 - 1)(\gamma + x_2) - \sqrt{[1 + (\alpha_2 - 1)(\gamma + x_2)]^2 - 4\gamma\alpha_2(\alpha_2 - 1)x_2}}{2\gamma(\alpha_2 - 1)}$$

$$a = \frac{(\alpha_2 - 1)\gamma + 1}{(\alpha_2 - 1)(1 - \gamma)}$$

$$b = \frac{(\alpha_2 - 1)\gamma - \alpha_2}{(\alpha_2 - 1)(1 - \gamma)}$$

Here it may be noted that the useful formula postulated by Saltonstall et al. (1983) for calculating the membrane area of binary permeation systems can readily be verified by Eq. 15.

Permeation Experiments on Hydrogen Recovery and Acid Gas Separation

Multicomponent gas separation experiments were performed in the laboratory to verify the mathematical model and to determine the feasibility of using the cellulose acetate membrane for H_2, CO_2, and H_2S separation. A reverse-osmosis, asymmetric, cellulose acetate hollow-fiber membrane was used in the experiments. To make the water-wet membrane suitable for gas permeation, however, it was necessary to dry the hollow fibers by a solvent exchange method to preserve the asymmetric structure of the membrane (MacDonald and Pan, 1974). The fiber has a thin outer skin supported by a porous structure of approximately 200 μm OD and 80 μm ID. To minimize gas consumption, all tests were performed on a miniature fiber module made of ten 36 cm long fibers in a U-loop configuration (N = 20 in Eq. 3), with the open ends of the fibers imbedded in a 3 cm long epoxy tube sheet. The module was housed in a 2.1 mm ID steel tube, in order to reduce the void space around the fibers and eliminate channeling of feed gas flow. During the test, the high-pressure feed gas was directed to flow through the shell side of the module at controlled pressure and temperature, and the permeate was withdrawn from the fiber openings on the tube sheet. The residue flow from the module was regulated by a flow controller, but the permeate back-pressure was controlled manually with a needle valve. The feed gas mixtures were made in the laboratory by blending the gas components. Gas chromatographs and mass-flow meters were used to measure gas compositions and flow rates.

H_2 recovery from purge gas of reactors

The economic and technical feasibility of the membrane process for hydrogen recovery has been successfully demonstrated by the commercialization of the well-known Monsanto permeators (Van Gelder, 1982). To determine the suitability of the asymmetric cellulose acetate membrane for similar applications, multicomponent permeation experiments were performed to simulate the recovery of hydrogen from the ammonia plant purge gas. The typical purge gas from an ammonia synthesis loop consists of 63% H_2, 21% N_2, 11% CH_4, 3% A, and 2% NH_3. As a high level of NH_3 (above 10 psi [68.9 kPa]) is detrimental to the cellulose acetate membrane, it was not included in the feed gas used in the experiment. For commercial application of the membrane, the ammonia in the purge gas can easily be reduced to a tolerable level by water absorption or by pressure swing adsorption using a silica gel adsorbent.

Excellent performance of the cellulose acetate membrane for hydrogen recovery was obtained in the permeation experiments. At 25°C, the membrane has a H_2/CH_4 selectivity of about 100. The typical test results for both countercurrent and cocurrent patterns are shown in Figures 2 and 3. As expected, the flow pattern has a negligible effect on the gas separation performance of the high-flux asymmetric membrane (Pan, 1983). The values predicted by the mathematical model using pure gas permeabilities are also shown in these figures. The agreement between the experimental data and the calculated values is good over a wide range of stage cuts. The discrepancy at stage cuts greater than 0.55, however, appears to be somewhat larger than the estimated experimental error of ±3.5%, and may be due to the fact that the mathematical assumption of negligible back-diffusion in the porous supporting layer of the membrane is not totally satisfied under extreme operating conditions. At high hydrogen

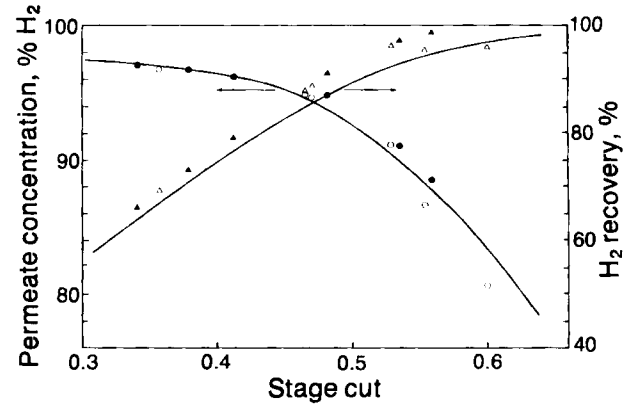

Figure 2. Performance of asymmetric cellulose acetate hollow-fiber membrane for hydrogen recovery from simulated purge gas of ammonia plant.

Feed: 6,964 kPa, 25°C, 51.78% H_2, 24.69% N_2, 19.57% CH_4, 3.96% A

Permeate: 1,123 kPa

Experimental data: ● ▲ countercurrent pattern; ○ △ cocurrent

—— calculated by mathematical model using pure-gas permeabilities:

H_2 permeability $Q/d = 2.84 \times 10^{-8}$ mol/m$^2 \cdot s \cdot$ Pa

Selectivity: H_2/CH_4 = 100, N_2/CH_4 = 1.04, A/CH_4 = 2.71

recovery (i.e., high stage cut), the major portion of the membrane area is exposed to the hydrogen-depleted feed-side stream, and the resulting low local permeate flux through the porous layer may not be high enough to totally overcome the back-diffusion from the bulk permeate stream toward the membrane skin. Such diffusion will tend to dilute and concentrate the local permeate concentration on the skin surface for the countercurrent and cocurrent flow patterns, respectively, resulting in the observed discrepancy between test data and calculated values at high hydrogen recovery. For most applications, however, the optimum recovery is likely to be less than 95% due to the high permeate purity or low membrane area requirement, and

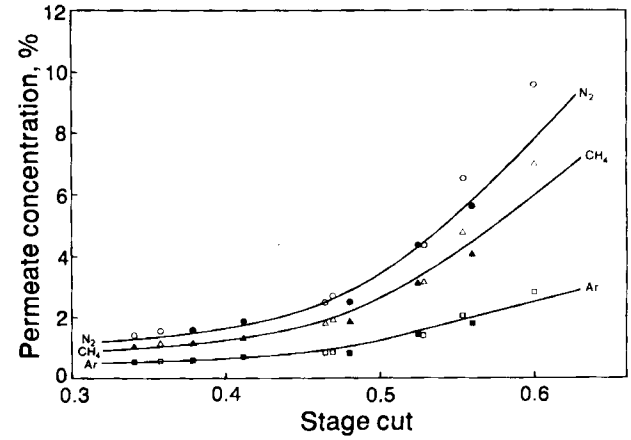

Figure 3. Effect of stage cut (permeate flow/feed flow) on impurity concentrations in permeate for hydrogen recovery from simulated purge gas of ammonia plant.

Operating conditions same as Fig. 2.

Experimental data: ● ▲ ■ countercurrent pattern; ○ △ □ cocurrent

—— calculated by mathematical model using pure-gas permeabilities, see Fig. 2

the present model should be adequate for calculating the performance of the asymmetric membrane.

While the present model has been verified by the experimental data shown in Figures 2 and 3, the same test results also provide solid evidence that conventional models for the symmetric membrane are not applicable to the high-flux asymmetric membrane. For example, at 0.55 stage cut, the test in the cocurrent mode yields a permeate stream with 973 kPa hydrogen partial pressure (86.6% in 1,123 kPa total pressure), and a residue stream with 612 kPa hydrogen partial pressure (8.8% in 6,964 kPa). Thus, at the residue end of the permeator, the hydrogen partial pressure on the permeate side is 1.6 times that on the feed side. Such results are not mathematically or physically possible according to conventional models whereby, in the absence of externally introduced permeate purge, the partial pressure of any permeating component in the bulk permeate stream can never be greater than that on the opposite feed side of the membrane.

Analysis of hydrogen recovery from purge gas

The test results clearly demonstrated the technical feasibility of the cellulose acetate membrane for hydrogen separation. The suitability of this membrane for hydrogen recovery from the reactor purge is analyzed below.

The purpose of venting the purge gas from the reactor recycle loop is to prevent continuing buildup of inert gases in the reactor. Therefore, a properly designed hydrogen recovery process should have a reject residue stream with the inert gas volume equal to that contained in the original purge stream prior to the installation of the hydrogen recovery unit. Most single-stage permeation processes, however, do not produce ultrahigh-purity hydrogen for recycle to the reactor, resulting in incomplete rejection of the inert gas. Under such conditions, it is necessary to increase the purge flow to the permeators, so that the volume of the inert gases contained in the increased residue flow is equal to that rejected by the original purge. The ratio of the necessary purge flow (after the installation of the hydrogen recovery unit) to the original purge flow is called purge factor. Clearly the larger the purge factor, the greater is the membrane area requirement. The purge factor generally increases with decreasing membrane selectivity and increasing hydrogen recovery, as shown in Figure 4, and plays an important role in determining the optimum membrane selectivity for hydrogen recovery. In the following analysis of the effect of membrane selectivity on membrane plant requirements, the permeability, Q/d, for hydrogen is assumed to be constant, and the variation of selectivity is due to the variation of the permeability for the inert gas (methane and nitrogen). This is a reasonable basis for the comparison of different asymmetric membranes, because the permeability, Q/d, to hydrogen of each membrane can, in principle, be controlled by varying the skin thickness, d, but the selectivity is an inherent property of the specific membrane.

Pan and Habgood (1974) have shown that for given feed flow and hydrogen recovery, the membrane area requirement generally decreases with decreasing membrane selectivity. This is due to the effect of an increased hydrogen permeation driving force across the membrane, resulting from lower hydrogen concentration in the permeate. The permeate compression power requirement, on the other hand, increases with decreasing selectivity, due to the larger permeate volume from increased permeation of the inert gas. In the case of hydrogen recovery from the reactor

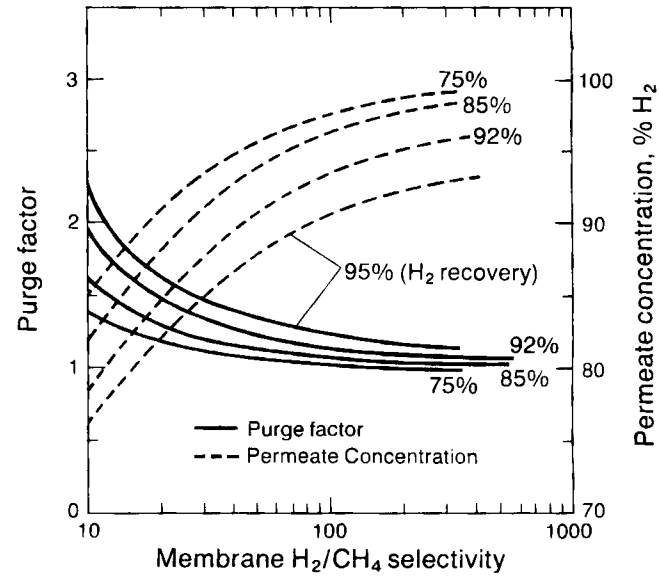

Figure 4. Effect of membrane selectivity on permeate concentration and purge factor in recovery of hydrogen from purge gas of ammonia plant.

Feed: 10,400 kPa, 32°C, 64% H_2, 21% N_2, 12% CH_4, 3% A
Permeate: 2,154 kPa
H_2 recovery = 100(1 − H_2 in permeator residue/H_2 in original purge prior to installation of permeators)

purge gas, these effects are further complicated by the purge factor. Decreasing the membrane selectivity decreases the membrane area requirement per unit feed flow, but it also increases the total feed flow to the membrane plant because of the increased purge factor, as discussed above. Hence, the purge factor tends to counteract the effect of selectivity on the membrane area requirement. The net result of these two opposing effects is shown by the solid lines in Figure 5. At high selectivities, the purge factor is always close to 1, and the membrane area is dependent mainly on selectivity (increasing selectivity increases area); but at low selectivities, the effect of the increased purge factor is more significant than that of selectivity, causing the required membrane area to increase with decreasing selectivity. This results in a minimum area requirement at an intermediate membrane selectivity. The role of the purge factor on the permeate compression power requirement, on the other hand, is relatively straightforward. Decreasing membrane selectivity increases the permeate volume for a given hydrogen recovery from a unit feed flow, and it also increases the total feed flow to the membrane plant due to the increased purge factor. Thus, the purge factor enhances the effect of membrane selectivity on the permeate compression power requirement, as shown by the broken lines in Figure 5.

Here it is important to note that the most desirable membrane selectivity is not necessarily the one with the minimum membrane area requirement. The optimum selectivity should result in a minimum combined cost of membrane area and permeate compression. The optimization of membrane selectivity requires knowledge of the relative costs of the membrane and the compression. In the absence of these cost data, however, the limits for optimum selectivity can still be established from the following consideration. It is clear from Figure 5 that the low limit of the desirable selectivity is around 20 and 40 (the selectivities corresponding to the minimum area requirement) for 95 and

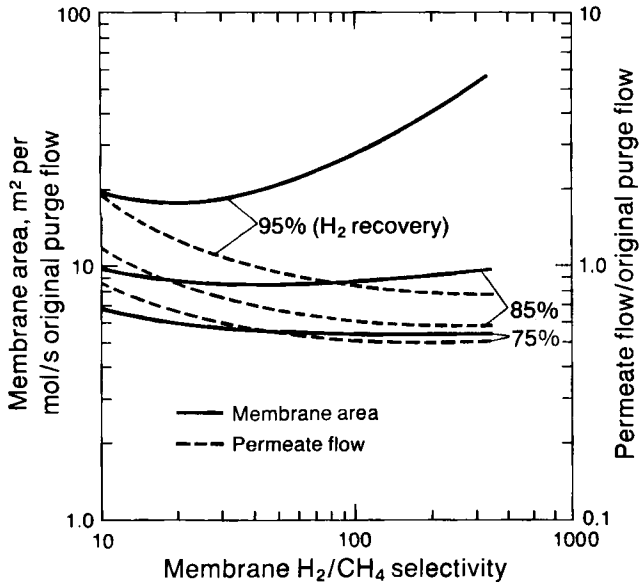

Figure 5. Effect of membrane selectivity on membrane area and permeate compression (proportional to permeate flow) requirements in recovery of hydrogen from purge gas of ammonia plant.

Feed: 10,400 kPa, 32°C, 64% H_2, 21% N_2, 12% CH_4, 3% A
Permeate: 2,154 kPa
H_2 permeability $Q/d = 3.36 \times 10^{-8}$ mol/m² · s · Pa

85% hydrogen recovery, respectively. This is because at lower selectivities both the membrane area and permeate compression power increase with decreasing selectivity. The high limit of the desirable selectivity is around 100, because at higher selectivities increasing the selectivity increases the membrane area significantly with only a negligible reduction in the permeate compression requirement. These selectivity limits match closely the selectivity of the cellulose acetate membrane (60 at 70°C and 100 at 25°C). Thus, the cellulose acetate membrane is ideally suited to the recovery of hydrogen from the reactor purge gas.

CO_2/H_2S separation from sour gas mixtures

The conventional amine absorption process has been widely used for the separation of CO_2 and H_2S from sour natural gas and the associated gas produced by CO_2-flooded enhanced oil recovery operations. However, the process becomes expensive for treating gases with high acid gas concentrations, because both the capital and energy consumption are proportional to the amount of acid gas to be removed. For a natural gas with 40% CO_2, approximately 15–20% of the salable methane will be consumed as fuel to operate the absorption process. On the other hand, membrane permeation is an efficient process for bulk separation of high-concentration CO_2 and H_2S, due to the existence of large permeation driving forces. Its separation efficiency, however, decreases with decreasing acid gas concentration in the feed. Therefore, the strengths and weaknesses of the membrane process are opposite to the amine absorption process. These two processes can complement each other to reduce the sour gas processing cost by using the membrane for bulk separation, followed by absorption for final cleanup. The permeation experiments carried out in this study are directed toward the development of this hybrid membrane/absorption process, and concern only the bulk separation of acid gas.

Extensive sour gas separation experiments were performed in the laboratory to study the permeation behavior of high-concentration CO_2 and H_2S and their interaction with other gas components. The typical test results are shown in Figures 6 and 7. At 10°C, the cellulose acetate membrane has an effective CO_2/CH_4 selectivity of 36 for mixed gas permeation. The continuous curves shown in these figures are calculated by the mathematical model using the permeabilities determined by matching the calculated values of the permeate composition and flow with the test data of a single experiment at an arbitrarily chosen stage cut. This procedure is necessary because the membrane permeabilities to the individual components in mixed-gas permeation are significantly different from the pure-component data. The observed permeabilities to methane and nitrogen are approximately twice that of their pure-gas values. Also, the strong pressure dependency of the permeabilities to CO_2 and H_2S observed in pure-gas permeability measurements is not present in mixed-gas permeation experiments. The increased membrane permeability to methane and nitrogen appears to be at variance with that predicted by the dual-mode sorption and transport model for mixed-gas permeation in unplasticized glassy polymers (Chern et al., 1983b), and is likely due to membrane plasticization by CO_2 and H_2S.

The close agreement between the experimental data and the calculated curves over a wide range of stage cuts shown in Figures 6 and 7 means that the mathematical model based on constant permeabilities determined by a single mixed-gas permeation experiment can be used to predict the performance of the cellulose acetate membrane for bulk separation of CO_2 and H_2S. However, the model is not expected to be accurate for the permeation process designed for the near-complete removal of large amounts of sour gas where the acid gas concentration in the residue is less than 1% of that in the feed. Under such conditions, a

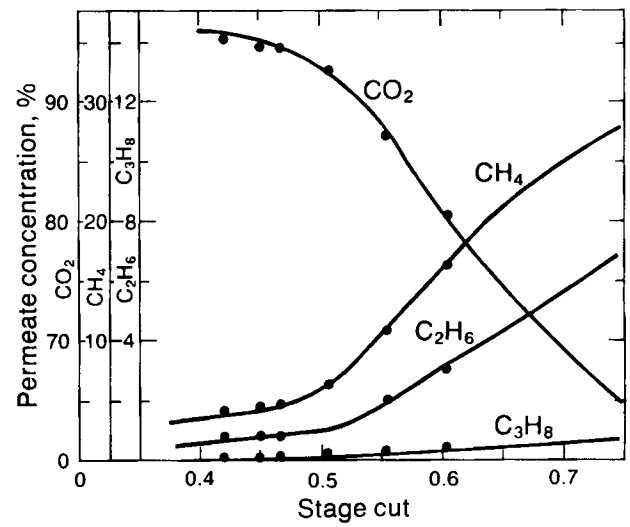

Figure 6. Performance of asymmetric cellulose acetate hollow-fiber membrane for CO_2 separation from hydrocarbon mixture.

Feed: 3,528 kPa, 10°C, 48.5% CO_2, 27.9% CH_4, 16.26% C_2H_6, 7.34% C_3H_8
Permeate: 92.8 kPa, countercurrent to feed
● experimental data
—— calculated by mathematical model using CO_2 permeability $Q/d = 1.34 \times 10^{-8}$ mol/m² · s · Pa
Selectivities: $CO_2/CH_4 = 36.0$, $C_2H_6/CH_4 = 0.275$, $C_3H_8/CH_4 = 0.0536$

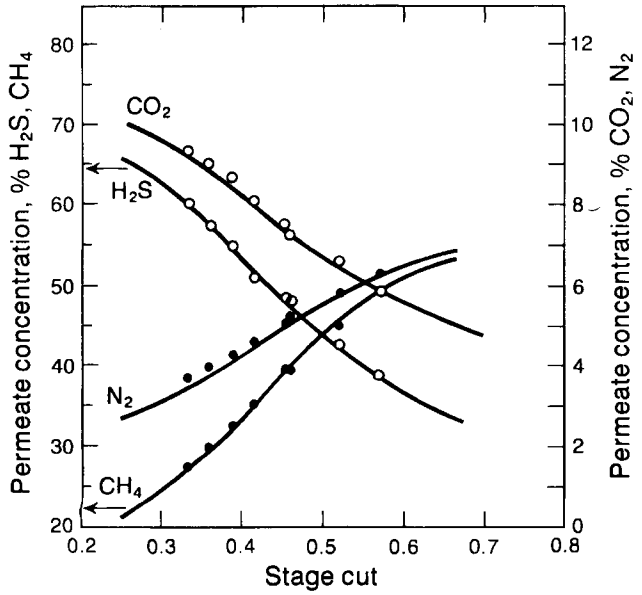

Figure 7. Performance of asymmetric cellulose acetate hollow-fiber membrane for H_2S/CO_2 separation from hydrocarbon mixture.

Feed: 5,245 kPa 50°C, 22.09% H_2S, 3.38% CO_2, 66.05% CH_4, 8.37% N_2, 0.11% C_2H_6
Permeate: 92.8 kPa, countercurrent to feed
● ○ experimental data
—— calculated by mathematical model using H_2S permeability $Q/d = 2.45 \times 10^{-8}$ mol/m² · s · Pa
selectivities: H_2S/CH_4 = 18.5, CO_2/CH_4 = 18.5, N_2/CH_4 = 1 (membrane not the same as that in Fig. 6)

valid mathematical model must take into account the effects of acid gas concentration on membrane permeabilities to methane and nitrogen.

Conclusions

1. The porous supporting layer of the asymmetric membrane will prevent the mixing of local permeate fluxes, giving rise to a cross-flow pattern with respect to the membrane skin, irrespective of the flow direction of the bulk permeate stream outside the porous layer. It has been shown experimentally that the conventional models for the countercurrent and cocurrent flow patterns are not applicable to the high-flux asymmetric membrane.

2. The mathematical model based on the cross-flow pattern can be used to calculate the performance of the high-flux asymmetric membrane. For the hollow-fiber membrane with significant permeate pressure buildup inside the fiber bore, an iteration method may be used to obtain the solution of the differential equations. For the special case of constant feed and permeate pressures, the membrane area requirement can be calculated by a simple algebraic formula using the permeate flow and composition.

3. The asymmetric cellulose acetate membrane has excellent permeation properties for hydrogen recovery and acid gas separation. In particular, the membrane selectivity for hydrogen is ideally suited to the recovery of hydrogen from plant offgases.

Acknowledgment

This work was done with financial support of Alberta Helium Ltd. (now International Permeation, Inc.) of Calgary, Alberta. The laboratory permeation experiments were performed by Earl Hadfield.

Notation

D_i = inside diameter of hollow fiber, m
D_o = outside diameter of hollow fiber, m
d = effective thickness of skin of asymmetric membrane, m
N = number of fibers in hollow-fiber module
P = feed-side pressure, Pa
p = permeate-side pressure, Pa
Q_1 = permeability to component 1, mol/m · s · Pa
Q_i = permeability to component i, mol/m · s · Pa
R = ideal gas constant
S = dimensionless membrane area
T = temperature, K
u = feed-side flow rate in hollow-fiber module, mol/s
u_c = feed-side flow at closed end of fiber (feed flow for cocurrent flow pattern, or residue flow for countercurrent flow pattern), mol/s
u_f = feed-side flow at feed inlet of hollow-fiber module, mol/s
$U = u/u_f$, dimensionless feed-side flow
$U_c = u_c/u_f$, dimensionless feed-side flow at closed end of fiber
v = bulk permeate flow rate, mol/s
x_{fi} = feed concentration of component i, mol frac
x_i = feed-side concentration of component i, mol frac
y_{fi} = local permeate concentration of component i on membrane surface at feed inlet, mol frac
y_i = local permeate concentration of component i on membrane surface, mol frac
$\bar{y}_i$ = permeate concentration of component i in bulk permeate stream, mol frac
y_n = local permeate concentration of component n (most or least permeable component) on membrane surface, mol frac
$y_o = \Sigma_1^n y_i/\alpha_i$
z = hollow fiber length variable, m

Greek letters

α_i = membrane selectivity for component i (permeability of component i/permeability of component 1)
α_n = membrane selectivity for component n (most or least permeable component)
γ = ratio of permeate pressure to feed pressure
θ = stage cut (ratio of permeate flow to feed flow)
μ = viscosity of gas mixture, Pa · s
μ_1 = viscosity of component 1, Pa · s

Literature cited

Berman, A. S., "Laminar Flow in Channels with Porous Walls," *J. Appl. Phys.*, **24,** 1232 (1953).

Blaisdell, C. T., and K. Kammermeyer, "Gas Separation through Expansible Tubing," *AIChE J.*, **18,** 1015 (1972).

———, "Countercurrent and Cocurrent Gas Separation," *Chem. Eng. Sci.*, **28,** 1249 (1973).

Boucif, N., A. Sengupta, and K. K. Sirkar, "Approximate Solutions for a Hollow-Fiber Gas Permeator with Countercurrent or Cocurrent Flow," *Symp. Gas Separation by Membranes,* AIChE Winter Meet., Atlanta (Mar., 1983).

Chern, R. T., W. J. Koros, E. S. Sanders, and R. Yui, "Second-Component Effects in Sorption and Permeation of Gases in Glassy Polymers," *J. Membr. Sci.*, **15,** 157 (1983a).

Chern, R. T., W. J. Koros, E. S. Sanders, S. H. Chen, and H. B. Hopfenberg, "Implications of the Dual-mode Sorption and Transport Models for Mixed Gas Permeation," *ACS Symp. Ser. No. 223,* **47** (1983b).

Hayara, K., T. Hakuta, and H. Yoshitome, "The Calculation of a Serial-Fed Gas Permeator System," *Separ. Sci. Tech.*, **20,** 403 (1985).

Hwang, S.-T., and K. Kammermeyer, *Membrane in Separation,* Wiley-Interscience, New York (1975).

MacDonald, W. R., and C. Y. Pan, "Method for Drying Water-Wet Membranes," U.S. Pat. 3,842,515 (1974).

Oishi, J., Y. Matsumura, K. Higashi, and C. Ike, "Analysis of a Gaseous Diffusion Separation Unit," *J. Atomic Energy Soc. (Japan),* **3,** 923 (1961); U.S. Atomic Energy Commission Report AEC-TR-5134.

Pan, C. Y., "Gas Separation by Permeators with High-Flux Asymmetric Membranes," *AIChE J.*, **29,** 545 (1983).

Pan, C. Y., and H. W. Habgood, "An Analysis of the Single-Stage Gaseous Permeation Process," *Ind. Eng. Chem. Fundam.* **13,** 323 (1974).
———, "Gas Separation by Permeation. I: Calculation Methods and Parametric Analysis," *Can. J. Chem. Eng.,* **56,** 197 (1978a).
———, "Gas Separation by Permeation. II: Effect of Permeate Pressure Drop and Choice of Permeate Pressure," *Can. J. Chem. Eng.,* **56,** 210 (1978b).
Perrin, J. E., and S. A. Stern, "Modeling of Permeators with Two Different Types of Polymer Membranes," *AIChE J.,* **31,** 1167 (1985).
Saltonstall, C. W., R. W. Lawrence, and D. Niu, "Calculation of Performance in Membrane Separation," AIChE Spring Nat. Meet. Houston (1983).
Shindo, Y., T. Hakuta, and H. Yoshitome, "Calculation Methods for Multicomponent Gas Separation by Permeation," *Separ. Sci. Tech.,* **20,** 445 (1985).
Stern, S. A., in *Industrial Processing with Membranes,* R. E. Lacey and S. Loeb, eds., Wiley-Interscience, New York (1972).
Stern, S. A., and S.-C. Wang, "Countercurrent and Cocurrent Gas Separation in a Permeator Stage. Comparison of Computation Methods," *J. Membr. Sci.,* **4,** 141, (1978).
Thorman, J. M., H. Rhim, and S.-T. Hwang, "Gas Separation by Diffusion through Silicone Rubber Capillaries," *Chem. Eng. Sci.,* **30,** 751 (1975).
Van Gelder, J. M., "Hydrogen Recovery from Ammonia Plant Purge Gas via Prism Separators," Tech. Conf. on Ammonia Fertilizer Technol., Beijing, China (Mar., 1982).
Walawender, W. P., and S. A. Stern, "Analysis of Membrane Separation Parameters. II: Countercurrent and Cocurrent Flow in a Single Permeation Stage," *Separ. Sci.,* **7,** 553 (1972).
Weller, S., and W. A. Steiner, "Separation of Gases by Fractional Permeation through Membranes," *J. Appl. Phy.,* **21,** 279 (1950a).
———, "Engineering Aspects of Separation of Gases—Fractional Permeation through Membranes," *Chem. Eng. Prog.,* **46,** 585 (1950b).

Manuscript received Feb. 28, 1986, and revision received June 5, 1986.